Biochimica et Biophysica Acta 1824 (2012) 533–541

Contents lists available at SciVerse ScienceDirect

Biochimica et Biophysica Acta

journal homepage: www.elsevier.com/locate/bbapap

QM/MM studies on the catalytic mechanism of Phenylethanolamine N-methyltransferase

Q.Q. Hou [a], J.H. Wang [a], J. Gao [a], Y.J. Liu [a,b,*], C.B. Liu [a]

[a] Key Lab of Colloid and Interface Chemistry, Ministry of Education, School of Chemistry and Chemical Engineering, Shandong University, Jinan, Shandong 250100, China
[b] Key Laboratory of Adaptation and Evolution of Plateau Biota, Northwest Institute of Plateau Biology, Chinese Academy of Sciences, Xining, Qinghai 810001, China

ARTICLE INFO

Article history:
Received 25 November 2011
Received in revised form 5 January 2012
Accepted 26 January 2012
Available online 3 February 2012

Keywords:
QM/MM
Epinephrine
Methyltransferase
Reaction mechanism
Mutation

ABSTRACT

Epinephrine is a naturally occurring adrenomedullary hormone that transduces environmental stressors into cardiovascular actions. As the only route in the catecholamine biosynthetic pathway, Phenylethanolamine N-methyltransferase (PNMT) catalyzes the synthesis of epinephrine. To elucidate the detailed mechanism of enzymatic catalysis of PNMT, combined quantum-mechanical/molecular-mechanical (QM/MM) calculations were performed. The calculation results reveal that this catalysis contains three elementary steps: the deprotonation of protonated norepinphrine, the methyl transferring step and deprotonation of the methylated norepinphrine. The methyl transferring step was proved to be the rate-determining step undergoing a SN2 mechanism with an energy barrier of 16.4 kcal/mol. During the whole catalysis, two glutamic acids Glu185 and Glu219 were proved to be loaded with different effects according to the calculations results of the mutants. These calculation results can be used to explain the experimental observations and make a good complementarity for the previous QM study.

1. Introduction

Epinephrine (EPI, also known as adrenaline), is a naturally occurring hormone. It is released from the adrenal gland within the central nervous system (CNS) [1,2]. Increased data has shown that epinephrine acts directly in controlling the cardiac excitability [3], blood pressure [3], vasodilation [3], respiration [4], and metabolism by stimulating the α and β receptors. Recently, it was also suggested that it may be extensively concerned with the degeneration of those neurons in the Alzheimer's disease [5,6].

Epinephrine is synthesized from amino acid tyrosine, which undergoes a series of intermediates catalyzed by different enzymes and ultimately evolves into epinephrine [7,8]. In the final step, Phenylethanolamine N-methyltransferase (PNMT) catalyzes the transfer of norepinphrine (NE) to epinephrine, utilizing the cofactor S-adenosyl-L-methionine (AdoMet) as a methyl group donor, [8] as depicted in Fig. 1. It is proved to be the key path for the formation of this neurotransmitter. Therefore, to elucidate the catalytic mechanism of PNMT is vital for the fundamental importance, and also sheds light on the design of new PNMT inhibitors.

Over decades, a variety of studies have addressed on the gene expression, mutagen, structure, and inhibitors design of PNMT. In 1959, Kirshner firstly identified that PNMT is responsible for the synthesis of epinephrine from norepinephrine [9]. Very recently, Axelrod demonstrated that PNMT in adult mammals was highly localized in the aderenal medulla [10]. Subsequently, an isotopic assay was applied in PNMT to measure the effects of various physiologic states and drugs on epinephrine biosynthesis [11–14]. In recent years a number of crystallographic studies have presented the static three-dimensional spatial arrangement of atoms of PNMT in complex with inhibitors [15–18]. On the basis of sequence analysis, PNMT belongs to the small molecule subfamily of methyltransferases (MTs) that use AdoMet as methyl group donor.

The crystal structure of human PNMT (hPNMT) was reported by Martin, [19] which is a ~31 kDa protein. There is an α/β domain in the polypeptide fold that combines with one central 7-stranded mixed β sheet and three helices. The crystal structures reveal that the substrate and cofactor are located on one edge of the β sheet. And several motifs form an extensive cover enclosing the binding sites. From the site-directed mutagenesis, several residues surrounding the active pocket such as Asp267, Glu219 and Glu185 have been identified, which play important roles in the catalysis.

Previous researches have provided much information. However, few studies have focused on the reaction mechanism of PNMT. Recently, the hybrid density functional theory method has been used to study the reaction mechanism of hPNMT [20]. In the calculations, three active site models were constructed of different size. In the small model, only the simplified coenzyme and substrate were included. In the larger model, some residues around the substrate were kept frozen at their crystallographic positions. Although these models proved that the methyl-transfer reaction occurs via a SN2

* Corresponding author at: Key Lab of Colloid and Interface Chemistry, Ministry of Education, School of Chemistry and Chemical Engineering, Shandong University, Jinan, Shandong 250100, China. Tel.: +86 531 88365536; fax: +86 531 88564464.
E-mail address: yongjunliu_1@sdu.edu.cn (Y.J. Liu).

1570-9639/$ – see front matter © 2012 Elsevier B.V. All rights reserved.
doi:10.1016/j.bbapap.2012.01.017

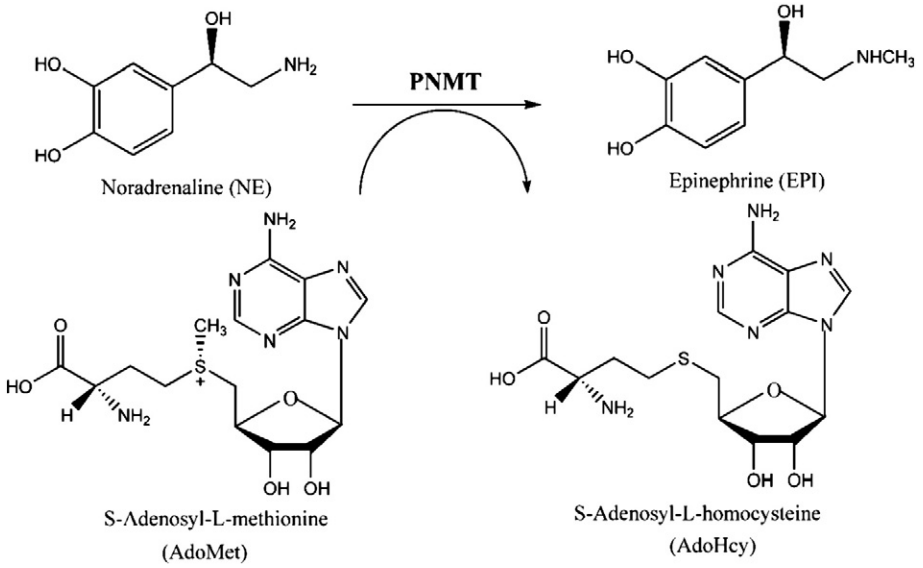

Fig. 1. Schematic showing of the chemical reaction catalyzed by PNMT. PNMT catalyzes the transfer of an activated methyl group from S-adenosyl-L-methionine (AdoMet) to the amine of norepinephrine (NE) forming epinephrine (EPI) and S-adenosyl-L-homocysteine (AdoHcy).

mechanism, different models undergo different paths with different barriers. Model C(H+) presented better results, but the model was not suitable for the study of subsequent proton transfer. In addition, the protein environment is usually considered to be significant for an enzyme catalysis, but this work did not involve the whole enzyme environment. Kamerlin and coworkers [21] proposed that simple models which ignore most parts of the enzyme and frozen the catalytic residues during the calculations could not adequately model the electrostatic environment of the real active site. There are still a number of intriguing questions that remain unsolved. For example, how many elementary steps does this reaction contain, the mechanistic details of the methyl group transfer process, and how the environments, especially the residues in or surrounding the active pocket, influence the catalytic reaction. Answers to these questions are not yet accessible by experimental approaches. Therefore, further theoretical study at the atomic level is highly desired.

Here, we present a comprehensive theoretical study on PNMT by using combined quantum mechanics and molecular mechanics (QM/MM) method, which has been successfully applied in the fields of extended systems, including enzymes [22–26]. But to the best of our knowledge, it has not been applied in the studies of PNMT. The basic idea of QM/MM is easy to understand. The whole system is partitioned into two regions that the reactive region (QM region) is treated quantum-mechanically and the outer region (MM region) is described by a classic force field. In this methodology, not only the chemical bond breaking and forming could be described, but also the effect of the total protein and solvent water could be taken into account [27–32]. The binding structure, possible mechanism, energetic details of intermediates and transition states, and the roles of key residues will be elucidated in this paper.

2. Computational details

2.1. Computational model

So far, there is no available crystal structure of PNMT ternary complex in the reactive state, as under the regular experimental conditions it would immediately lead to the product state. In our calculations, the initial model was prepared on the basis of X-ray crystal structure of hPNMT in complex with S-adenosyl-L-homocysteine (AdoHcy) and the inhibitor SK&F 29661 (PDB ID: 1HNN), [19] as shown in Fig. 2(a). In the crystal, there are two almost identical monomers in the asymmetric unit, so one monomer is chosen as the computational model. AdoHcy was amended to AdoMet by adding one methyl group on the sulfur atom based on the geometry parameters of AdoMet bound to PNMT reported by Gee and coworkers [16]. The norepinphrine molecule was separately optimized at the B3LYP/6–31G(d) level with the Gaussian 03 package [33] and then deposited into the active pocket in place of the inhibitor using the Autodock program [34]. Then the complete enzyme–cofactor–substrate model was solvated into a water sphere of 30 Å radius centered on the nitrogen atom of norepinphrine. All hydrogen atoms were added by the HBUILD facility in the CHARMM 22 [35]. Three sodium ions were also added at random positions to neutralize the system. SHAKE algorithm [36] was used to constrain the stretching of bonds involving hydrogen atoms. The PROPKA method [37,38] was used to adjust the protonation states of ionizable residues. In the QM region, the pKa values of Glu219 and Glu185 calculated by the PROPKA method were 6 and 7, respectively, thereby both of them were assigned to the deprotonated forms under the standard assay conditions of pH 8.0. For noradrenaline, the amine would be expected to be protonated. The Mulliken charge parameters of the substrate were derived from the QM(B3LYP) calculations. The resulting complex contains 14,927 atoms, including PNMT protein, AdoMet, norepinphrine, 3598 water molecules, and 3 sodium ions. A total of 800 ps molecular dynamics simulation was performed to equilibrate the system and the last snapshot was selected as the starting structure for the QM/MM optimizations, as shown in Fig. 3. All the above procedures were accomplished with the CHARMM22 all-atom force field program [39].

2.2. QM/MM calculations

Following the equilibration described earlier, the QM region was chosen to include residues Glu185, Glu219, Tyr35, protonated norepinphrine, a part of AdoMet and two water molecules, for a total of 81 QM atoms. The total charge of this region is 0. The rest of the model atoms were assigned to the MM part. The QM/MM interface was treated by a pseudobond reaction coordinate approach [40,41]. The QM part was treated at the B3LYP/6–31G(d) level and the MM part was described at the CHARMM22 force field. During the QM/MM geometry optimizations, the QM region and the MM atoms within a distance of 10 Å centered on the N atom of norepinphrine were allowed to relax, whereas the remaining MM atoms were fixed. A

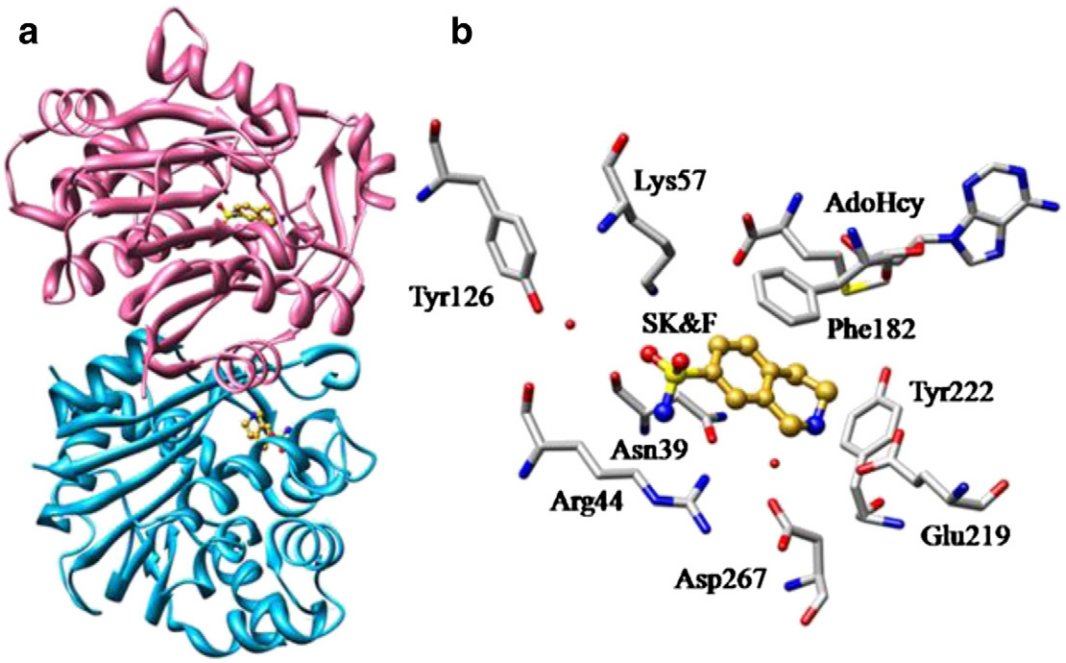

Fig. 2. (a) Crystal structure of PNMT (PDB code: 1HNN); (b) Structure of the active pocket taken from the crystal.

standard electronic embedding scheme [42] was employed to describe the electrostatic interactions between the QM region and MM region. The point charges of all the MM atoms were incorporated into one electron Hamiltonian of the QM treatment to avoid the polarization effects, and hydrogen link atom method was used to satisfy the valences. The QM/MM calculations were performed with ChemShell [43] which combines Turbomole [44] and DL-POLY [45] for density functional theory and MM calculations, respectively. The QM/MM-scanned energy mapping method was employed to describe the reaction path by representing a discrete number of structures. A geometry optimizer of hybrid delocalized internal coordinates (HDLC) in ChemShell was used to perform optimizations, which uses the quasi-Newton limited memory Broyden–Fletcher–Goldfarb–Shanno (L-BFGS) algorithm to search for minima, and the partitioned rational function optimization (P-RFO) algorithm for transition states. The L-BFGS optimizer starts from a unit Hessian and applies the BFGS updated on the fly using the history of the optimization, and this method is well suited for optimization problems with a large number of variables. The P-RFO method can find transition states by following eigenmodes of the Hessian, and the transition states are characterized by a single negative eigenvalue [43]. Finally, to obtain accurate energies, single-point QM/MM calculations at larger basis set 6–31++G(d,p) were performed. All the energies reported herein were corrected by zero-point vibrational effects.

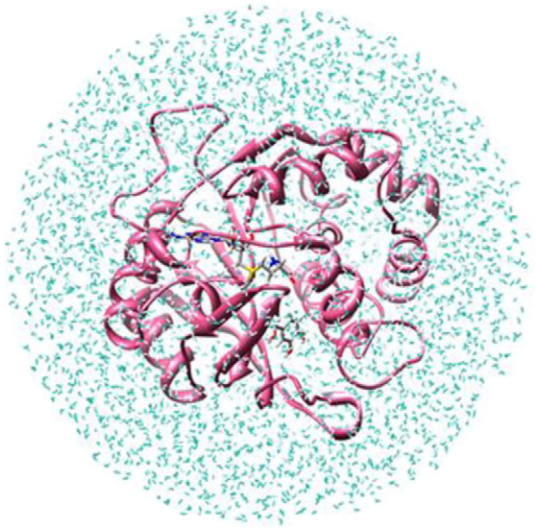

Fig. 3. The final solvated model of PNMT, after treatment with CHARMM package.

3. Results and discussion

3.1. Structure of enzymic ternary complex

The initial crystal structure [19] is shown in Fig. 2(a), with the inhibitor (SK&F 29661) and cofactor product (AdoHcy) binding in the active pocket. SK&F 29661 is a common inhibitor for PNMT which is composed of a tetrahydroisoquinoline system with a sulfonamide substituted at 7 position. Fig. 2(b) shows the active pocket and surrounding residues. Glu219 forms one hydrogen bond to the aliphatic amino directly, while Asp267 form one hydrogen bond to the aliphatic amino through a mediated-water molecule. Asn39 and Phe182 connect to the aliphatic amino by hydrogen-bonding and π–π interactions. Arg44, Tyr123 and Lys57 interact with the two oxygen atoms. Overall, these surrounding residues are believed to be catalytically important for PNMT.

In the QM/MM model, the protonated norepinphrine was used to substitute the inhibitor. The optimized structure taken from the reactive pocket of PNMT is shown in Fig. 4. Compared with the crystal structure including the inhibitor, the active pocket is located at the same position as the protein, but the binding mode is a little bit different. In the optimized geometry, the methyl group presents excellent direction towards to the protonated amino group. The nitrogen atom of amino is positioned by Tyr35 and Tyr222 through a mediated-water molecule, and the hydrogen atom is stabilized by a hydrogen bond to Glu219 and Glu185 through a mediated-water molecule. In the side chain hydroxyl group, the oxygen atom forms a hydrogen bond to a water molecule and Asp267, and the hydrogen atom is hydrogen bonded to the residue Glu219. Another residue

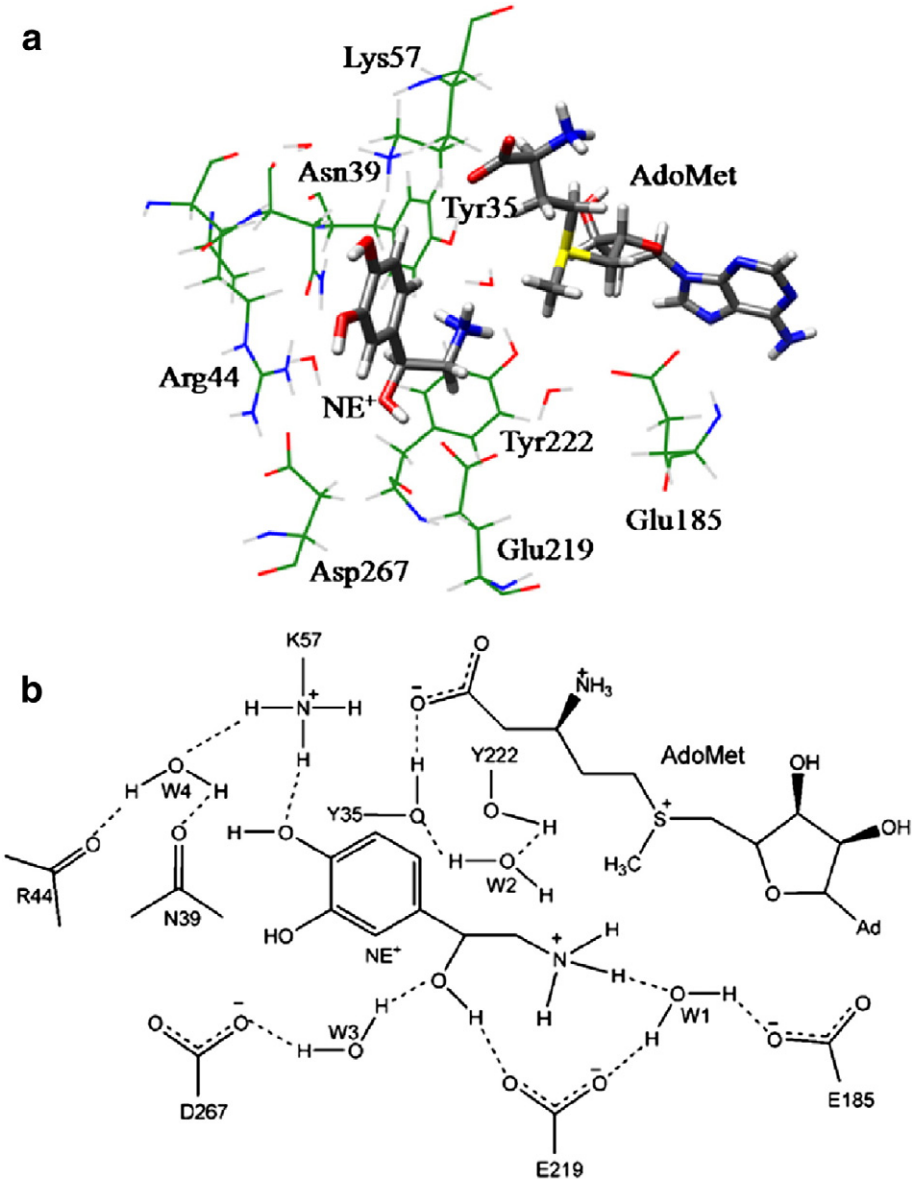

Fig. 4. (a) The active site structure of PNMT at its initial state after QM/MM optimization; (b) The skeleton drawing.

Lys57, near the 4-OH group, makes a strong interaction with the oxygen atom. Arg44 and Asn39 are located at the side of the active pocket. Then a large hydrogen bonding network is formed in the active region and the substrate is tightly bound to the coenzyme and protein by these hydrogen bonds, which would be responsible for the critical near-attack reactive conformation effect. This structure is used as the initial reactive state for the QM/MM calculations of the reaction mechanism.

3.2. Reaction paths

In this subsection, we provide the calculation results of reaction mechanism. This catalysis is supposed to occur through three steps as illustrated in Fig. 5, i.e., the protonated amino deprotonating step, the methyl transferring step, and the methylated norepinephrine deprotonating step. First, the protonated amino loses a proton to Glu185, yielding the neutral norepinephrine. Then, the methyl group transfers from the sulfur atom of coenzyme AdoMet to the nitrogen atom of norepinephrine, with the concomitant conversion of AdoMet to AdoHcy. Last, the protonated epinephrine loses one proton to form the final product. As can be seen from our model, a mediated water functions as a bridge for the proton transferring to Glu219.

The optimized structures along the PNMT catalytic process are demonstrated in Figs. 6 and 7. In the first step, a proton of the protonated norepinephrine moves to Glu185 through a water bridge, and the neutral norepinephrine which behaves as the methyl acceptor as the next step is formed. This process undergoes a low energy barrier of 5.4 kcal/mol. In the second step, the methyl transfer is described as a typical SN2 process. As can be seen from the structure of the intermediate **IM1** in Fig. 6, the methyl donor and acceptor present a very right order that the lone pair of electrons of the amino nitrogen point to the methyl carbon of AdoMet. The distance between the methyl carbon and the N atom of NE is 3.77 Å, and the angle of S(AdoMet)…CH_3…N(NE) is 152.9°. The positively charged sulfur atom of AdoMet also largely facilitates the methyl transfer. In **TS2** (shown in Fig. 7), the methyl group is almost planar placed between the donor and the acceptor atoms. The distances of S(AdoMet)…C and C…N(NE) are 2.19 and 2.47 Å, respectively. For the angle of S(AdoMet)…CH_3…N(NE), it increases as the reaction progresses and has a maximal value of 169.37°, which is a nearly linear arrangement. In addition, the methyl group has a net positive charge of 0.26.

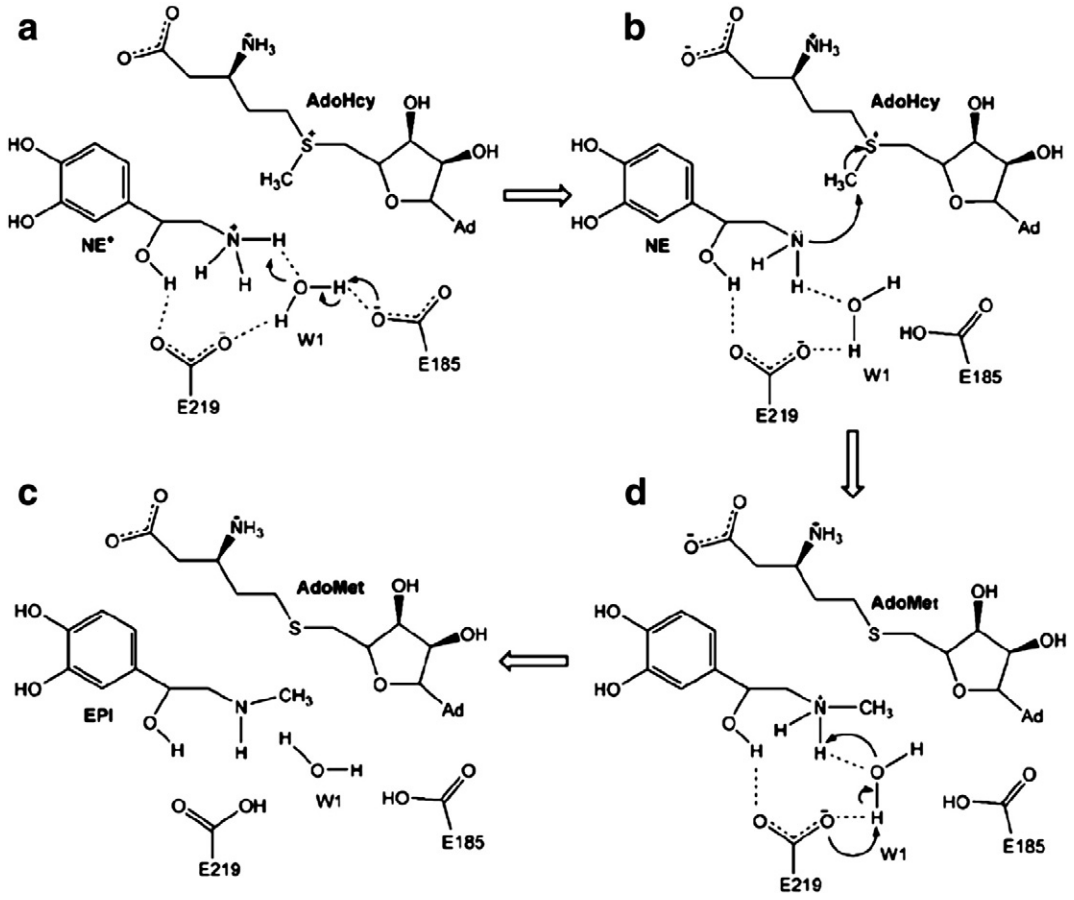

Fig. 5. The proposed reaction path for PNMT. (a) Deprotonation. A proton transfers from the protonated amine to Glu185 via a bridging water. (b) Nucleophilic attack. The methyl group transfers from AdoHcy to NE. (c) Deprotonation. A proton transfers from the methylated NE to Glu219 via a bridging water. (d) Products of the reaction, EPI and AdoMet are generated. Ad refers to the adenine ring of AdoMet and AdoHcy.

Frequency calculations give the unique imaginary frequency of 161i cm^{-1} for **TS2**. All these data suggest an inherent characteristic of SN2 mechanism. Then the methyl group successfully transfers to the nitrogen of NE, and the coenzyme AdoMet converts to AdoHcy simultaneously. A new hydrogen bond forms between the sulfur atom and Tyr35 though a mediated water molecule, stabilizing the coenzyme. This methyl-transfer process suffers an energy barrier of 16.4 kcal/mol and an exothermicity of 48.2 kcal/mol. The barrier is consistent within the framework of transition state theory with the experimentally observed k_{cat} [46]. Then the positive charge on N will facilitate the proton transfer to form the final product EPI. As shown in our mechanism, the last step is a water-assisted proton transfer from methylated NE to Glu219, which is considered to be a concerted mechanism that one hydrogen of methylated amino group transfers to the bridge water, and simultaneously one hydrogen of water moves to the carboxylate ions of Glu219. The bond distance of H(NE)…O(W1) has been shortened from 1.63 in **IM2** to 0.99 Å in **P**, meanwhile the distance of H(W1)…O(Glu219) has changed from 1.86 to 1.10 Å. The **TS3** has an imaginary frequency of 138i cm^{-1} and the calculated energy barrier is 4.7 kcal/mol. Finally, the product EPI is formed and released from the active site. The corresponding energy profile along the reaction path is presented in Fig. 8.

For the first step, we also attempted another pathway in which Glu219 behaves as the proton acceptor. But the protonated glutamic acid on residue Glu219 was not stable enough to be obtained. The proton atom always spontaneously transfers to Glu185 and the same product as previous was formed. As can be seen from Fig. 8, for the methyl transferring step, it proceeds with an exothermicity of 48.2 kcal/mol. In an effort to elucidate the origins of the high exothermicity, firstly, we compared the QM region structures of **IM1** and **IM2**. In these two states, the structures and positions of the surrounding residues only changed a little, and one water molecule (W2) moved obviously. Then, in **IM2** a new hydrogen bond formed between the sulfur atom and Tyr35 by the aid of W2, stabilizing the coenzyme. To exam the energetic contribution of W2, it was partitioned into the MM region. But the obtained energy barriers only changed by 1~2 kcal/mol. It could be concluded that there were no structural movements that would contribute to the high exothermicity. Then two models of different size were constructed based on our QM/MM model, and their relative energies were calculated at the B3LYP/6–31G(d) level with the Gaussian 03 package [33]. In the small model, only the substrate (norepinphrine) and the coenzyme (AdoMet) were considered, while the other surrounding residues were removed. In the large model, all the residues in the QM region of our QM/MM calculations (Glu185, Glu219, Tyr35, W1 and W2) were included. In the two models, the energy barriers of the methyl transfer step were almost the same (11.0 and 11.2 kcal/mol) as that of QM/MM model, but the exothermic values were greatly different, which were −15.0 and −61.0 kcal/mol for the small and larger models, respectively, as shown in Fig. S1. These results agree quite well with the results of F. Himo [20] and our QM/MM calculations. In F. Himo's work, the high exothermic values were also obtained from the large models (model B and model C), and the lower exothermic value from the small model (model A). It suggests that residues Gln185, Glu219, Tyr35 and two water molecules exhibit great influences on the reaction energies. By checking the electronic changes of **IM1** and **IM2**, we found that the positive charge on the sulfur atom of AdoMet has transferred to the nitrogen of norepinphrine

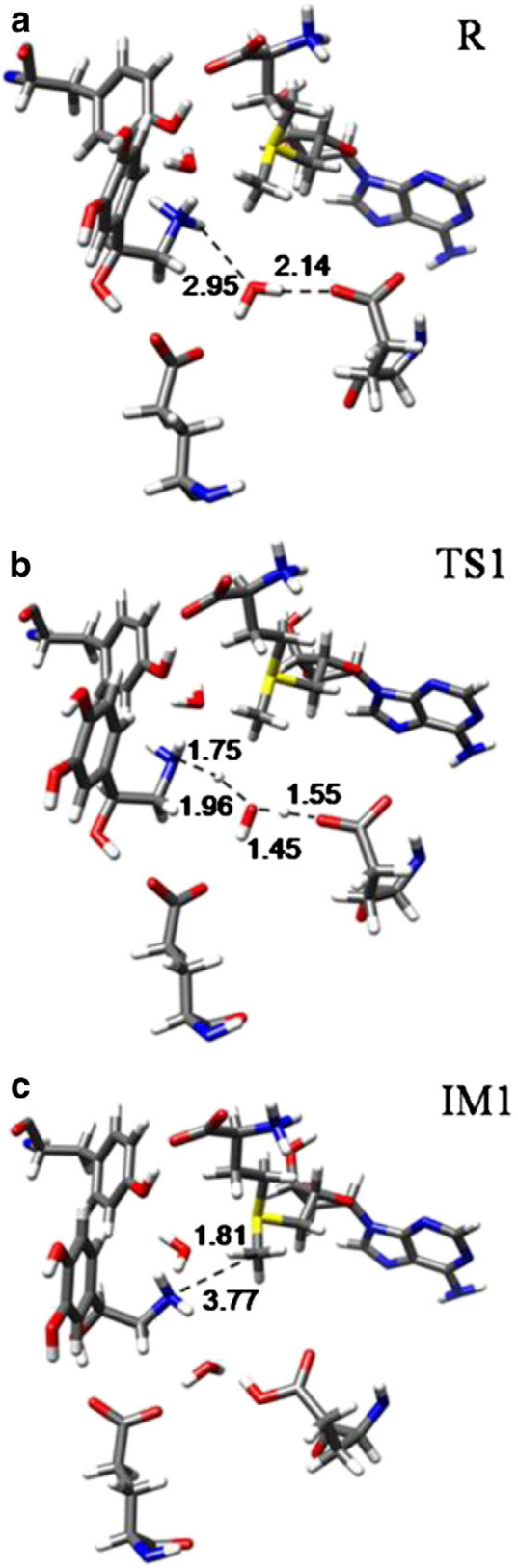

Fig. 6. Optimized structures of reactant (R), Transition state (**TS1**), Intermediate (**IM1**). Distances are given in Å.

during the methyl transfer step. And the positive charge on nitrogen atom of **IM2** is dispersed by the surrounding residues, especially Glu185, Glu219, and Adp267. Overall, our results have confirmed the remarkable role of the protein environments and solvent molecules in stabilizing the system.

It should be noted that the starting structure used for the QM/MM calculations on wild-type PNMT was constructed completely based on the X-ray crystal structure. As described above, we have performed an 800 ps MD simulation, achieving a change in energy of <0.001 kcal/mol and a RMS gradient of <0.001 kcal/mol·Å. However, different starting structures may affect the energy barriers but not the reaction mechanism. More recently, total of 11 different initial structures taken from MD simulations were used to calculate the reaction energy path for histone lysine methyltransferases (HKMTs) by Zhang and coworkers [47]. Their QM/MM calculations yielded a consistent mechanistic picture for the reaction and the fluctuation of free energy barriers was only ±1.1 kcal/mol. Furthermore, Xiong and coworkers [48] also examined the possible barrier fluctuation for one step of their enzymic reaction which was only 0.2 kcal/mol. Concluded from these previous studies, the barrier fluctuation has a strong connection with the geometric parameters associated with the reaction coordinate, more similar to the values of the geometric parameters with the corresponding average value, and closer to the energy barrier calculated with this snapshot to the average value of the energy barriers calculated with all the snapshots. To check the possible barrier fluctuation of our system, 800 ps MD simulations on the structure **IM1** were further performed, and a stable MD trajectory was obtained. The final snapshot was taken as the initial structure to repeat the QM/MM calculations for the proton transfer step as the previous calculations. At the same level, the activation barrier was calculated to be 17.1 kcal/mol which is 0.5 higher than the previous one. So, one snapshot close to the average values of the geometric parameters taken from MD simulation is reliable for the QM/MM optimization and mechanism calculations.

Overall, the QM/MM calculation result was found to be in relatively better agreement with the experiments than the work of F. Himo [20]. In their initial structures prepared for calculations, the protonated state the substrate was not obtained, because during the optimization, a proton moved immediately from the amino group to Glu185. Model B and model C were devised to represent the whole process of the catalysis. In model B, two elementary reactions were included which were methyl transfer and proton transfer. But in the later step, the proton transferred directly to Glu219 but not via the bridge water. In model C, the intermediate of methylated norepinphrine was not found, and the result was that the methyl transfer was concerted with the proton transfer. The mechanism derived from their calculation was a little different from ours, and we ascribe these to the different calculating models. In these QM studies, the cluster models were used for simplification, and the protein environment was considered using solvation calculations in a polarizable dielectric medium. But in our QM/MM calculations, the actual protein environment of PNMT is accounted for the catalytic mechanism. The important residues are included in the QM region and all the residues within a distance of 10 Å centered on the N atom of norepinphrine are flexible during the calculations, which enable us to model the reactive biomolecular systems at a reasonable effort. It is inspiring to see that our QM/MM results show a remarkable effect of the protein environment on the rate-determining reaction.

3.3. Analysis of the enzymatic environment contribution

There was a notable experimental phenomenon that the mutation of Glu185 to Gln decreased the catalytic rate constant (k_{cat}) of the enzyme by about 280-fold (0.01 min^{-1} vs 2.8 min^{-1}), but the mutation of Glu219 to Gln increased k_{cat} a little (2.9 min^{-1} vs 2.8 min^{-1}) [46]. Although much information has been gained from these mutagenesis results, the different roles of residues Glu185 and Glu219 are still unclear at atom level. To further elucidate such differences in catalysis, we carried out the QM/MM calculations on the basis of Glu185Gln

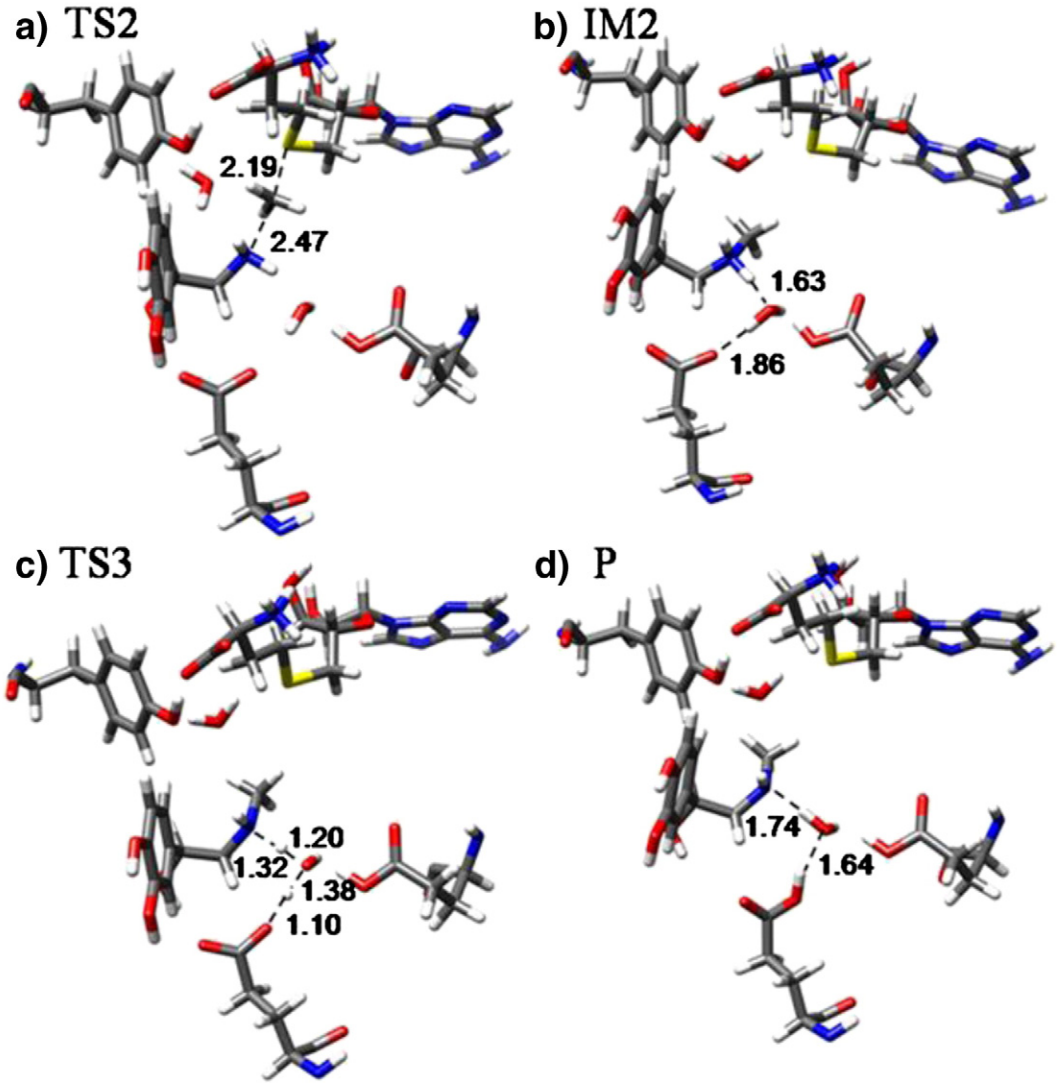

Fig. 7. Optimized structures of reactant (**TS2**), Transition state (**IM2**), intermediate (**TS3**) and product (P). Distances are given in Å.

and Glu219Gln mutants. Mutations by VMD, MD simulations at the CHARMM22 force field were firstly performed, and then geometrical optimization was carried out at the same QM/MM level of theory as for the wild enzyme.

In experiments, E185Q mutants had the same K_m value as the wild-type hPNMT but extremely lower k_{cat} value. The rate-determining step was studied and the QM/MM optimized geometries for the Glu185Gln mutant are depicted in Fig. 9. Compared with the geometries of **IM1** (in Fig. 6) associated with the wild enzyme, E185Q mutation presents obvious structural changes in the active

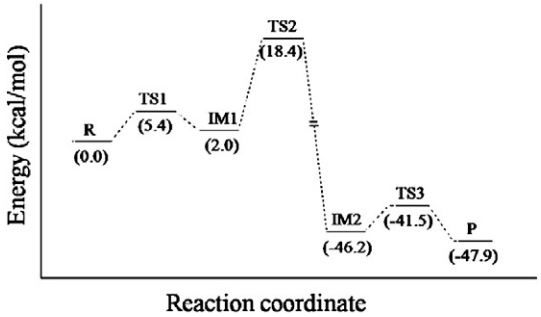

Fig. 8. Energy profile of the PNMT catalytic process.

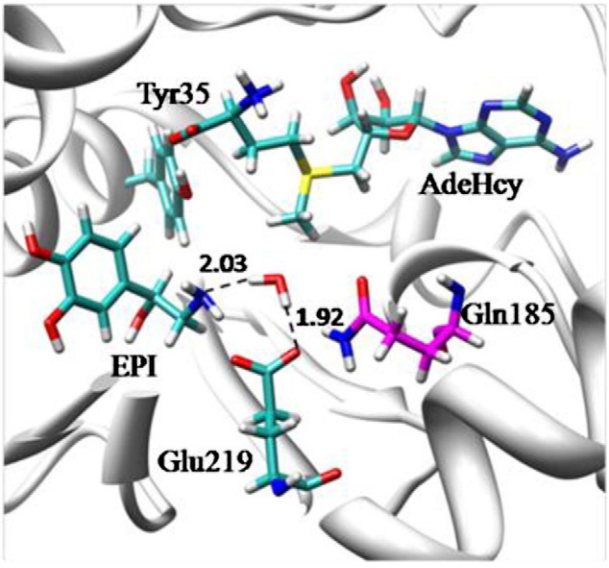

Fig. 9. QM/MM optimized active structure of enzyme mutation Glu185Gln.

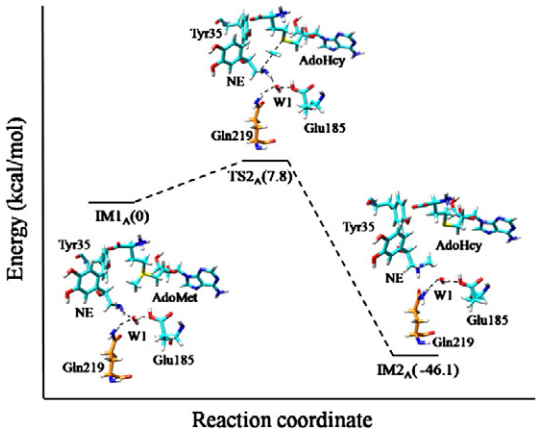

Fig. 10. Energy profile and optimized structures of intermediate (**IM1**$_A$), transition state (**TS2**$_A$) and intermediate (**IM2**$_A$) for mutation Glu219 in the methyl transferring step.

site. The hydrogen bond between the bridge water and residue 185 no longer exists. It is important to note that the bridge water is sandwiched between the methyl group and the amino. As a result the methyl-transfer path will be blocked compulsively. This is why the mutant of Gln185 had a lower k_{cat} value than that of wild enzyme.

Besides Glu185, another key residue taking part in the catalysis is Glu219. The site-directed mutagenesis results have shown that Glu219Gln had little effect on the k_{cat} value. Fig. 10 clearly displays the QM/MM optimized geometries and energy profile of the mutant Glu219Gln on the rate-determining reaction step. In the intermediate **IM1**$_A$, the near-attack reactive conformers is formed, which is similar with the reactant **IM1** of the wild-type enzyme. The bridge water still forms two hydrogen bonds between Gln219 and Glu185. The methyl donor and acceptor present favorable direction to each other for the methyl transfer. Similar with the wild-type enzyme, the methyl transfer undergoes a SN2 mechanism with an energy barrier of 7.8 kcal/mol. Frequency calculations give the unique imaginary frequency of 136i cm^{-1} for **TS2**$_A$. For the second step of proton transfer, **IM2**$_A$ undergoes a very small activation energy barrier to generate the final product **P**$_A$ (Fig. S2). Thus, in the case of the Glu219Gln mutant, the catalytic reaction proceeds successfully.

4. Conclusions

In the present study, the detailed mechanism of Phenylethanolamine N-methyltransferase (PNMT) was investigated by using combined quantum-mechanical/molecular-mechanical (QM/MM) approaches. The catalysis consists of three elementary steps, and the methyl transferring step is proved to be the rate-determining step undergoing a SN2 mechanism with an energy barrier of 16.4 kcal/mol at the QM/MM B3LYP/6–31++G(d,p)//CHARMM22 level of theory. In the active site, Glu219, Glu185, Tyr35, and two crystal water molecules are found to have the function to stabilize the transition state. Two glutamic acids of Glu185 and Glu219 have taken part in the catalysis, but played different roles. In the first step, Glu185 behaves as the proton acceptor, and the neutral substrate is formed. In the last step, Glu219 gets a proton from the protonated EPI, and the catalytic reaction is completed. Both of them could be the target residues for mutation to change the efficiency of PNMT.

Acknowledgements

This work was supported by the National Natural Science Foundation of China (21173129), and Graduate Innovation Foundation of Shandong University (yyx10025).

Appendix A. Supplementary data

Supplementary data to this article can be found online at doi:10.1016/j.bbapap.2012.01.017.

References

[1] L.M. Gunne, Relative adrenaline content in brain tissue, Acta Physiol. Scand. 56 (1962) 324–333.
[2] R.W. Fuller, Pharmacology of brain epinephrine neurons, Annu. Rev. Pharmacol. Toxicol. 22 (1982) 31–55.
[3] J.M. Saavedra, H. Grobecker, J. Axelrod, Adrenaline-forming enzyme in brainstem: elevation in genetic and experimental hypertension, Science 191 (1976) 483–484.
[4] A.B. Rothballer, The effects of catecholamines on the central nervous system, Pharmacol. Rev. 11 (1959) 494–547.
[5] W.J. Burke, H.D. Chung, R. Strong, M.B. Mattammal, G.L. Marshall, R. Nakra, G.T. Grossberg, J.H. Haring, T.H. Joh, Central Nervous System Disorders of Aging: Clinical Intervention and Research, Raven Press, New York, 1988, pp. 41–70.
[6] B.P. Kennedy, T. Bottiglieri, E. Arning, M.G. Ziegler, L.A. Hansen, E. Masliah, Elevated S-adenosylhomocysteine in Alzheimer brain: influence on methyltransferases and cognitive function, J. Neural Transm. 111 (2004) 547–567.
[7] J. Axelrod, Noradrenaline: fate and control of its synthesis, Science 19 (1971) 1251–1254.
[8] J. Minson, I. Llewellyn-Smith, A. Neville, P. Somogyi, J. Chalmers, Quantitative analysis of spinally projecting adrenaline-synthesising neurons of C1, C2 and C3 groups in rat medulla oblongata, J. Auton. Nerv. Syst. 30 (1990) 209–220.
[9] N. Kirshner, M. Goodall, The formation of adrenaline from noradrenaline, Biochim. Biophys. Acta 24 (1959) 658–659.
[10] J. Axelrod, Purification and properties of phenylethanolamine-N-methyl transferase, J. Biol. Chem. 237 (1962) 1657–1660.
[11] W.E. Bondinell, F.W. Chapin, J.S. Frazee, G.R. Girard, K.G. Holden, C. Kaiser, C. Maryanoff, C.D. Perchonock, G.W. Gessner, J.P. Hieble, L.M. Hillegass, R.G. Pendleton, J.L. Sawyer, Inhibitors of phenylethanolamine N-methyltransferase and epinephrine biosynthesis: a potential source of new drugs, Drug Metab. Rev. 14 (1983) 709–721.
[12] R.E. Toomey, J.S. Horng, S.K. Hemrick-Luecke, R.W. Fuller, α-Adrenoreceptor affinity of some inhibitors of norepinephrine N-methyl-transferase, Life Sci. 29 (1981) 2467–2472.
[13] M. Goldstein, M. Saito, J.Y. Lew, J.P. Hieble, R.G. Pendleton, The blockade of alpha2-adrenoceptors by the PNMT inhibitor SK & F 64139, Eur. J. Pharmacol. 67 (1980) 305–308.
[14] G.L. Grunewald, V.H. Dahanukar, R.K. Jalluri, K.R. Criscione, Synthesis, biochemical evaluation, and classical and three-dimensional quantitative structure-activity relationship studies of 7-substituted-1,2,3,4-tetrahydroisoquinolines and their relative affinities toward phenylethanolamine N-methyltransferase and the α2-adrenoceptor, J. Med. Chem. 42 (1999) 118–134.
[15] F.M. McMillan, J. Archbold, M.J. McLeish, J.M. Caine, K.R. Criscione, G.L. Grunewald, J.L. Martin, Molecular recognition of sub-micromolar inhibitors by the adrenaline synthesising enzyme PNMT, J. Med. Chem. 47 (2004) 37–44.
[16] C.L. Gee, N. Drinkwater, J.D.A. Tyndall, G.L. Grunewald, Q. Wu, M.J. McLeish, J.L. Martin, Structure of hPNMT with inhibitor 3-fluoromethyl-7-trifluoropropyl-THIQ and AdoHcy, J. Med. Chem. 50 (2007) 4845–4853.
[17] N. Drinkwater, C.L. Gee, M. Puri, K.R. Criscione, M.J. McLeish, G.L. Grunewald, J.L. Martin, Molecular recognition of physiological substrate noradrenaline by the adrenaline synthesising enzyme PNMT and factors influencing its methyltransferase activity, Biochem. J. 422 (2009) 463–471.
[18] N. Drinkwater, H. Vu, K.M. Lovell, K.R. Criscione, B.M. Collins, T.E. Prisinzano, S.A. Poulsen, M.J. McLeish, G.L. Grunewald, J.L. Martin, Fragment-based screening by X-ray crystallography, MS and isothermal titration calorimetry to identify PNMT (phenylethanolamine N-methyltransferase) inhibitors, Biochem. J. 431 (2010) 51–61.
[19] J.L. Martin, J. Begun, M.J. McLeish, J.M. Caine, G.L. Grunewald, Getting the adrenaline going: crystal structure of the adrenaline-synthesizing enzyme PNMT, Structure 9 (2001) 977–985.
[20] P. Georgieva, Q. Wu, M.J. McLeish, F. Himo, The reaction mechanism of phenylethanolamine N-methyltransferase: a density functional theory study, Biochim. Biophys. Acta 1794 (2009) 1831–1837.
[21] S.C.L. Kamerlin, Z.T. Chu, A. Warshel, On catalytic preorganization in oxyanion holes: highlighting the problems with the gas-phase modeling of oxyanion holes and illustrating the need for complete enzyme models, J. Org. Chem. 75 (2010) 6391–6401.
[22] B.L. Grigorenko, M.S. Shadrina, I.A. Topol, J.R. Collins, A.V. Nemukhin, Mechanism of the chemical step for the guanosine triphosphate (GTP) hydrolysis catalyzed by elongation factor Tu, Biochim. Biophys. Acta, Proteins Proteomics 1784 (2008) 1908–1917.
[23] D. Bellocchi, A. Macchiarulo, A. Carotti, R. Pellicciari, Quantum mechanics/molecular mechanics (QM/MM) modeling of the irreversible transamination of L-kynurenine to kynurenic acid: the round dance of kynurenine aminotransferase II, Biochim. Biophys. Acta, Proteins Proteomics 1794 (2009) 1802–1812.
[24] D. Riccardi, S. Yang, Q. Cui, Proton transfer function of carbonic anhydrase: insights from QM/MM simulations, Biochim. Biophys. Acta, Proteins Proteomics 1804 (2010) 342–351.
[25] R.B. Wu, S.L. Wang, N.J. Zhou, Z.X. Cao, Y.K. Zhang, A proton-shuttle reaction mechanism for histone deacetylase 8 and the catalytic role of metal ions, J. Am. Chem. Soc. 132 (2010) 9471–9479.

[26] J.E. Basner, S.D. Schwartz, How enzyme dynamics helps catalyze a reaction in atomic detail: a transition path sampling study, J. Am. Chem. Soc. 127 (2005) 13822–13831.
[27] H.M. Senn, W. Thiel, QM/MM methods for biomolecular systems, Angew. Chem. Int. Ed. 48 (2009) 1198–1229.
[28] J.L. Gao, S.H. Ma, D.T. Major, K. Nam, J.Z. Pu, D.G. Truhlar, Mechanisms and free energies of enzymatic reactions, Chem. Rev. 106 (2006) 3188–3209.
[29] Q. Cui, M. Karplus, Catalysis and specificity in enzymes: a study of triosephosphate isomerase (TIM) and comparison with methylglyoxal synthase (MGS), Adv. Protein Chem. 66 (2003) 315–372.
[30] J.L. Gao, D.G. Truhlar, Quantum mechanical methods for enzyme kinetics, Annu. Rev. Phys. Chem. 53 (2002) 467–505.
[31] M.J. Field, P.A. Bash, M. Karplus, A combined quantum-mechanical and molecular mechanical potential for molecular dynamics simulations, J. Comput. Chem. 11 (1990) 700–733.
[32] A. Warshel, M. Levitt, Theoretical studies of enzymic reactions: dielectric, electrostatic and steric stabilization of the carbonium ion in the reaction of lysozyme, J. Mol. Biol. 103 (1976) 227–249.
[33] M.J. Frisch, G.W. Trucks, H.B. Schlegel, G.E. Scuseria, M.A. Robb, J.R. Cheeseman, J.A. Montgomery, T. Vreven, K.N. Kudin, J.C. Burant, J.M. Millam, S.S. Iyengar, J. Tomasi, V. Barone, B. Mennucci, M. Cossi, G. Scalmani, N. Rega, G.A. Petersson, H. Nakatsuji, M. Hada, M. Ehara, K. Toyota, R. Fukuda, J. Hasegawa, M. Ishida, T. Nakajima, Y. Honda, O. Kitao, H. Nakai, M. Klene, X. Li, J.E. Knox, H.P. Hratchian, J.B. Cross, V. Bakken, C. Adamo, J. Jaramillo, R. Gomperts, R.E. Stratmann, O. Yazyev, A.J. Austin, R. Cammi, C. Pomelli, J.W. Ochterski, P.Y. Ayala, K. Morokuma, G.A. Voth, P. Salvador, J.J. Dannenberg, V.G. Zakrzewski, S. Dapprich, A.D. Daniels, M.C. Strain, O. Farkas, D.K. Malick, A.D. Rabuck, K. Raghavachari, J.B. Foresman, J.V. Ortiz, Q. Cui, A.G. Baboul, S. Clifford, J. Cioslowski, B.B. Stefanov, G. Liu, A. Liashenko, P. Piskorz, I. Komaromi, R.L. Martin, D.J. Fox, T. Keith, Al M.A. Laham, C.Y. Peng, A. Nanayakkara, M. Challacombe, P.M.W. Gill, B. Johnson, W. Chen, M.W. Wong, C. Gonzalez, J.A. Pople Gaussian03; Gaussian, Inc.: Wallingford, CT, 2004.
[34] G.M. Morris, D.S. Goodsell, R.S. Halliday, R. Huey, W.E. Hart, R.K. Belew, A.J. Olson, Automated docking using a Lamarckian genetic algorithm and empirical binding free energy function, J. Comput. Chem. 19 (1998) 1639–1662.
[35] A.D. MacKerell Jr., D. Bashford, M. Bellott, R.L. Dunbrack Jr., J.D. Evanseck, M.J. Field, S. Fischer, J. Gao, H. Guo, S. Ha, D. Joseph-McCarthy, L. Kuchnir, K. Kuczera, F.T.K. Lau, C. Mattos, S. Michnick, T. Ngo, D.T. Nguyen, B. Prodhom, W.E. Reiher, III, B. Roux, M. Schlenkrich, J.C. Smith, R. Stote, J. Straub, M. Watanabe, J. Wiorkiewicz-Kuczera, D. Yin, M. Karplus, All-atom empirical potential for molecular modeling and dynamics studies of proteins, J. Phys. Chem. B 102 (1998) 3586–3616.
[36] J.P. Ryckaert, G. Ciccotti, H.J.C. Berendsen, Numerical integration of the cartesian equations of motion of a system with constraints: molecular dynamics of n-alkanes, J. Comput. Phys. 23 (1977) 327–341.
[37] H. Li, A.D. Robertson, J.H. Jensen, Very fast empirical prediction and rationalization of protein pKa values, Proteins: Struct. Funct. Bioinf. 61 (2005) 704–721.
[38] D.C. Bas, D.M. Rogers, J.H. Jensen, Very fast prediction and rationalization of pKa values for protein-ligand complexes, Proteins: Struct. Funct. Bioinf. 73 (2008) 765–783.
[39] B.R. Brooks, R.E. Bruccoleri, B.D. Olafson, D.J. States, S. Swaminathan, M. Karplus, CHARMM: a program for macromolecular energy, minimization, and dynamics calculations, J. Comput. Chem. 4 (1983) 187–217.
[40] Y. Zhang, T. Lee, W. Yang, A pseudobond approach to combining quantum mechanical and molecular mechanical methods, J. Chem. Phys. 110 (1999) 46–54.
[41] Y. Zhang, Improved pseudobonds for combined ab initio quantum mechanical/molecular mechanical methods, J. Chem. Phys. 122 (2005) 024114.
[42] D. Bakowies, W. Thiel, Hybrid models for combined ɋuantum mechanical and molecular mechanical approaches, J. Phys. Chem. 100 (1996) 10580–10594.
[43] P. Sherwood, A.H. de Vries, M.F. Guest, G. Schreckenbach, C.R.A. Catlow, S.A. French, A.A. Sokol, S.T. Bromley, W. Thiel, A.J. Turner, S. Billeter, F. Terstegen, S. Thiel, J. Kendrick, S.C. Rogers, J. Casci, M. Watson, F. King, E. Karlsen, M. Sjøvoll, A. Fahmi, A. Schäfer, C. Lennartz, QUASI: a general purpose implementation of the QM/MM approach and its application to problems in catalysis, J. Mol. Struct. (Theochem) 632 (2003) 1–28.
[44] R. Ahlrichs, M. Bar, M. Haser, H. Horn, C. Kolmel, Electronic structure calculations on workstation computers: the program system turbomole, Chem. Phys. Lett. 162 (1989) 165–169.
[45] W. Smith, T.R. Forester, DL_POLY_2.0: a general-purpose parallel molecular dynamics simulation package, J. Mol. Graph. 14 (1996) 136–141.
[46] C.L. Gee, J.D.A. Tyndall, G.L. Grunewald, Q. Wu, M.J. McLeish, J.L. Martin, Binding mode of methyl acceptor substrates to the adrenaline-synthesizing enzyme phenylethanolamine N-methyltransferase: implications for catalysis, Biochemistry 44 (2005) 16875–16885.
[47] P. Hu, Y. Zhang, Catalytic mechanism and product specificity of the histone lysine methyltransferase SET7/9: an ab initio QM/MM-FE study with multiple initial structures, J. Am. Chem. Soc. 128 (2006) 1272–1278.
[48] Y. Xiong, J.J. Liu, G.F. Yang, C.G. Zhan, Computational determination of fundamental pathway and activation barriers for acetohydroxyacid synthase-catalyzed condensation reactions of α-keto acids, J. Comput. Chem. 31 (2010) 1592–1602.